Glass from the Cretaceous/Tertiary boundary in Haiti

Haraldur Sigurdsson*, Steven D'Hondt*, Michael A. Arthur*, Timothy J. Bralower†, James C. Zachos‡, Mickey van Fossen§ & James E. T. Channell§

* Graduate School of Oceanography, University of Rhode Island, Narragansett, Rhode Island 02882, USA
† University of North Carolina, Chapel Hill, North Carolina 27599, USA
‡ University of Michigan, Ann Arbor, Michigan 48109, USA
§ University of Florida, Gainesville, Florida 32611, USA

Tektite-like glasses preserved at the Cretaceous/Tertiary boundary at Beloc in Haiti provide clear evidence of an impact event. The glass composition suggests that the impact occurred on a continental shelf region, generating a silica-rich glass with chemical composition that reflects the melting of continental crustal rocks, and a calcium-rich glass produced by the fusion of marl sediments. These findings indicate that catastrophic release to the atmosphere of 10^{15} moles of CO_2 from vaporized marl occurred during the impact.

THE global event that marks the Cretaceous/Tertiary (K/T) boundary has left a striking signature of worldwide mass extinctions of marine biota and a pronounced geochemical anomaly in the sedimentary record, including enrichment of platinum-group elements such as iridium. Hypotheses put forward to account for these phenomena include the impact of a large asteroid on the Earth[1], and a pulse of severe volcanism[2,3]. Because of poor preservation of K/T boundary sediments, however, neither volcanic nor impact-derived glassy materials, such as tephra or tektites, have hitherto been found to provide unambiguous evidence of the nature of the catastrophic event or the chemical composition of the source region.

The thin band of claystone that marks the K/T boundary in continental and ocean sediments contains microspherules, which have been considered by some to be support of the impact hypothesis[4–6], whereas others have interpreted the spherules as authigenic in origin[3,7,8]. In Colorado and New Mexico, the K/T boundary sediments contain 0.1-mm kaolinite microspherules[7,8] which coexist with 0.6–0.7-mm shocked quartz minerals in the boundary clay, inconsistent with simultaneous fallout of these two particle types of widely different diameter from the same plume; thus the fallout origin of these small spherules is questionable. It has been suggested that the spherules result from deposition of secondary minerals in vesicles in originally glassy materials[9] and that the precursor to the K/T boundary claystone was glass[10]. Several workers have concluded, on the other hand, that the microspherules and particles are products of authigenic growth, due to diagenetic alteration of glassy material of impact or volcanic origin[7,8,11,12]. Others have proposed that the spherules are the direct result of impact, formed by solidification of impact melt[4], but the preservation of the materials has hitherto been too poor to arrive at definitive conclusions. On the basis of geochemical data, the terrain of the impact site has been alleged to be mainly oceanic crust of basaltic composition[12–14], but a more silicic source has also been suggested[5].

We document well preserved tektite-like spherules from a glass-rich layer at the K/T boundary in deep-water carbonate sediments in the Beloc region of Haiti, where the boundary deposit forms a layer 10–50 cm thick containing 25% glass spherules from 1 to 6 mm in diameter. The Haiti glasses are among the earliest preserved glasses on Earth and the oldest known impact glasses. The large size of the spherules and their occurrence in a relatively thick layer may be an indication of the close proximity of this outcrop to the source region. The coarse glass-bearing layer contains shocked quartz grains[15] and an iridium anomaly has also been reported at this level[16].

Stratigraphy

Within the sequence of deep-water carbonates and marls in the Beloc formation on the southern peninsula of Haiti[14,15], the K/T boundary interval is clearly marked by the glass-bearing layer. This layer directly overlies uppermost Maastrichtian limestones and chalks of *Abathomphalus mayaroensis* and *Micula murus* foraminiferal and nannofossil zones. It is immediately overlain by 5-cm basal Palaeocene PO (*Guembelitria cretacea*) foraminiferal zone sediments. Within 1.1 m of the top of the glass-bearing unit, typical *Parvularugoglobigerina eugubina* zone taxa first appear (*P. eugubina, Eoglobigerina eobulloides, Eoglobigerina moskvini*). The nannofossil *Biscutum romeinii* first appears 6.75 m above the glass-bearing horizon, which places the interval above that datum in the *B. romeinii* subzone of the earliest Palaeocene NP1 nannofossil zone[17,18]. Throughout the lowermost Palaeocene interval at this sequence, both nannofossil and foraminiferal results indicate very high sedimentation rates and a large amount of sedimentary reworking. The presence of an extended *Micula murus* zone (26.5–30 mm) and pre-boundary 29R palaeomagnetic interval (26 m) at the Beloc section suggests that the uppermost Maastrichtian part of the sequence is chronostratigraphically complete on 100-kyr timescales[19–21].

Petrology of glasses

The glass-bearing rock is pale brown to buff in colour, containing abundant smectite-coated glassy spherules in a silty marl of carbonate (42%) and smectite clay. The spherules make up approximately 25% of the rock, but originally the glass probably constituted about half of the rock, as the smectite is its alteration product. The 1–6-mm-diameter glasses are generally spherical, although ellipsoidal, elongated, tear-drop and bar-bell forms are also present, resembling splash-form tektites (Fig. 1*a*). They have a very smooth outer shell of light grey to brownish smectite of variable thickness (<1 mm), which also forms smectite vesicle infillings inside the spherules. Beneath the smectite shell, the exposed black glass surface has pits, fine ridges and furrows, probably produced after deposition and during the alteration process from glass to smectite (Fig. 1*b*). The smooth, spherical smectite shell probably represents the original morphology of the glass spherule. About 2% of the glasses are amber to yellowish in colour and more vesicular than the black glasses. The yellowish glass also occurs as thin (50–150 μm) schlieren or streaks within the black glass (Fig. 1*c*).

The spherules are mostly massive and entirely crystal-free, consisting of pale brown glass in thin section. The total lack of crystals or microlites in the glass is of great importance with regard to their origin—they thus resemble tektite glasses, which are typically crystal-free, and are unlike volcanic glasses, which

invariably contain either phenocrysts or microlites of high-temperature minerals. This petrographic distinction from volcanic glasses is even more striking when we consider that the andesitic volcanic rocks or magmas that broadly correspond to the Beloc glasses in chemical composition are typically very crystal-rich. This seriously calls into question any fractionation mechanism involving crystal separation as the process responsible for the observed chemical range in the Beloc glasses. The Beloc glasses contain vesicles of diameter 0.05–0.2 mm. In some spherules the vesicles are very rare (<5 vol%) and small, whereas the yellow glasses have up to 30% vesicularity. Some spherules are glass bubbles, consisting of a relatively thin-walled glass sphere filled with smectite. In addition to the smectite, some vesicles are filled by massive crystals of white barytes.

Chemical composition

The glasses range from 44–68% SiO_2 and form well defined compositional trends (Fig. 2). When plotted on mixing diagrams, the glasses define a linear relationship (Fig. 3), consistent with the mixing of two endmembers. The black glassy spherules are the dominant endmember, with about 66–68% SiO_2, enriched in alkalis and slightly enriched in alumina. The other endmember is the rare amber to yellowish glass, Ca-rich (30 wt%) and low in silica (SiO_2 44%), which also occurs as isolated fragments and as streaks in some black glassy spherules, similar to schlieren commonly observed in tektites (Fig. 1*c*). The high-Ca endmember is enriched in MgO. As is evident from their high oxide totals (mean 99.85 ± 0.5 wt%), the Beloc glasses are very volatile-poor, in contrast to the hydrous character of volcanic glass shards found in deep-sea sediments. Unlike the hydrated glass contained in volcanic ash layers in deep-sea sediments, the Beloc glasses have resisted hydration. They resemble tektites in this respect, where the anhydrous nature of the glass renders it a relatively stable structure and impregnable to hydration.

The black Beloc glasses have major- and trace-element composition very similar to the upper continental crust and thus resemble the composition of a wide variety of rock types, including the HNa/K australite tektites[22], calc-alkaline andesites, certain deep-sea turbidites[23], argillites, shale and mudrock. The only known entirely glassy rocks of this composition, however, are tektites. The black Beloc glasses have higher alkalis than terrestrial andesites and much higher potassium than HNa/K australites. The MgO content of Beloc glasses is considerably lower than in both australites and terrestrial andesites, and consequently the FeO/MgO ratio in the Beloc glasses is unusually high (1.8–2.4), compared to the others (1.5). Alumina is significantly lower in Beloc glasses than in terrestrial andesites and australites, by ~2 wt%, whereas CaO is somewhat higher. The high-Ca glasses present in the Beloc layer have no chemical or petrographic equivalent among terrestrial igneous rocks, but show some similarities to HNa/K australites and upper Eocene impact microspherules[24].

The trace-element distribution in a bulk sample of the black Beloc glasses (Table 1; Fig. 4) is broadly similar to that of the upper continental crust, with a high content of incompatible elements and a strong enrichment in light-rare-earth elements (REE) compared to chondrite (La/Yb = 7.7). HNa/K australites, Ivory Coast tektites and calc-alkaline andesites have

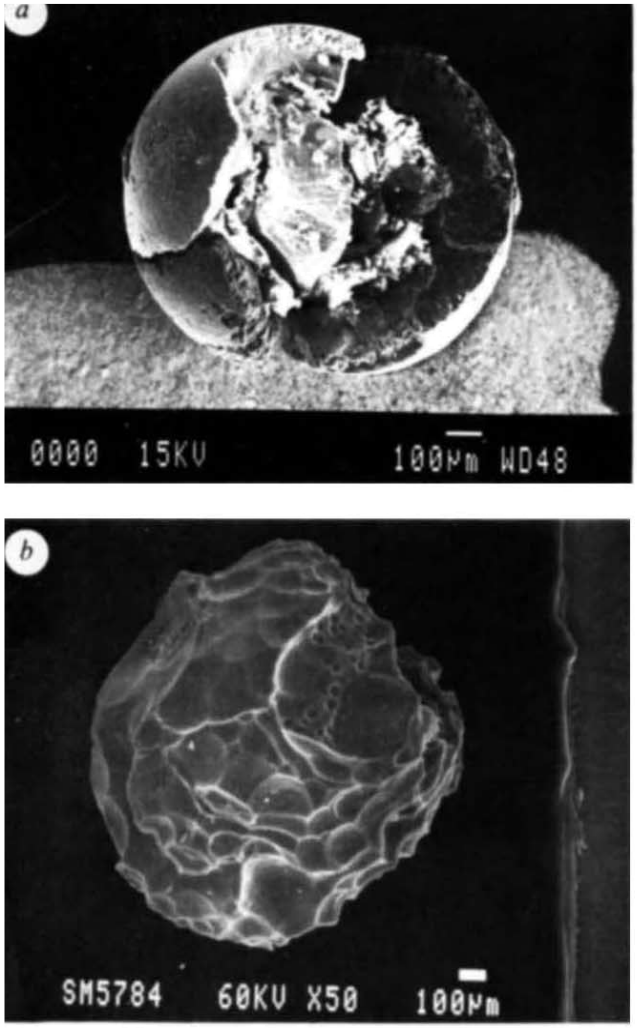

FIG. 1 *a*, Scanning electron micrograph of glass spherule from the K/T boundary at Beloc in Haiti. A smooth smectite shell encloses the glass. *b*, Scanning electron micrograph of glass spherule after removal of the smectite layer. *c*, Backscatter electron micrograph of polished thin section of a Beloc glass spherule. The glass is inhomogeneous, with elongated lighter grey streaks or bands of Ca-rich and silica-poor glass, typically 50–150 μm in width, within the dominant black high-silica glass. Scale bars, 100 μm.

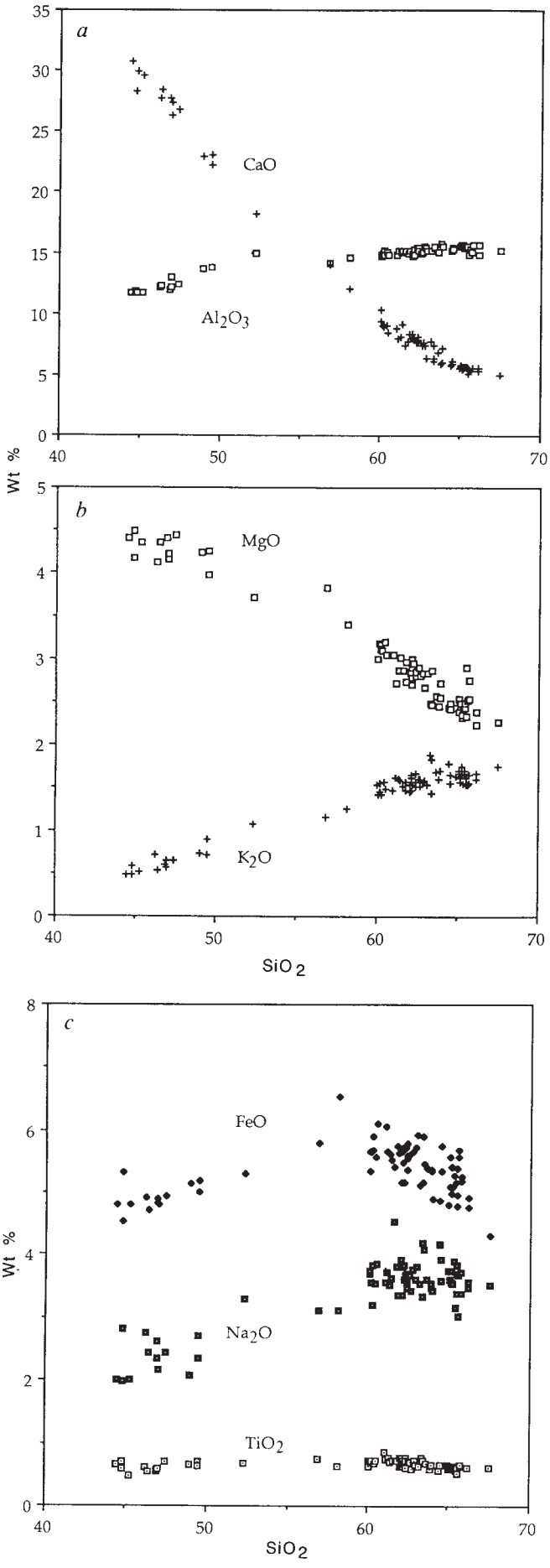

comparable REE patterns[22,25]. The Beloc glasses have unusually high Th/U ratio (5.8) compared to andesites, however, and are further distinguished from andesites by the very high K/Cs ratio (13,500). The Cs-depletion in the glasses relative to continental crust and volcanic-arc rocks may be an indication of Cs-loss during fractional vaporization from a tektite liquid. The Beloc glasses have rather low Cr and Ni concentrations, comparable to modavite tektites[26] and terrestrial andesite[27]. The Beloc and moldavite tektite glasses thus differ from australites and Ivory Coast tektites, which have Cr and Ni contents that are an order of magnitude higher and which may have been contaminated by the asteroid body that generated these impact melts.

Origin of compositional range

Silicate-liquid compositional trends such as those exhibited by the Beloc glasses could result from fractional crystallization of magma, mixing of two magmas, fractional vaporization of an impact melt at superliquidus temperatures, or the mixing of impact melts derived from a heterogeneous source. A magmatic fractional crystallization origin for the observed trend is excluded because of the total absence of crystals from the glasses and the difference between typical magmatic compositional trends and those of the Beloc glasses. The very high CaO content (up to 30.7 wt%) observed in the Beloc glass low-silica endmember is unknown for volcanic rocks. A magma mixing origin is also discounted on the basis of these observations.

One factor that can lead to compositional diversity among tektite glasses is selective fractional vaporization. The observed order of volatility in silicate melts under conditions of high temperature is $K_2O > SiO_2 > Na_2O > FeO > TiO_2 > MgO > Al_2O_3 > CaO$[22,26,28]. Volatility of alkalis is dependent on oxygen fugacity, and is reduced at atmospheric pressure[29]. If the compositional range of Beloc glasses were due to fractional vaporization of the melt, then the most silicic and high-alkali glass could represent the closest approximation to the source composition, and the low-alkali and low-silica glass would have suffered greatest fractional vaporization. The observed enrichment and depletion factors of the Beloc glasses are not, however, consistent with fractional vaporization. Whereas CaO shows the increase expected for a refractory oxide, the relative order of enrichment of the other oxides is $K_2O > Na_2O > SiO_2 > Al_2O_3 > TiO_2 > FeO > MgO > CaO$, inconsistent with the oxide sequence predicted for fractional vaporization. Thus Al_2O_3 seems to behave as a slightly volatile oxide, whereas experimental studies clearly demonstrate its refractory behaviour. Furthermore, the degree of fractional vaporization required to account for the trends is excessive. Assuming that Ca is incompatible in the vapour (refractory during volatilization), production of the high-Ca glass would require 85% volatilization of the high-silica glass. Considering the high degree of volatilization implied by the Ca variation, it would indeed be surprising that the alkalis were not depleted to greater extent in the high-Ca glass. Furthermore, as shown in Fig. 3, plots of the ratios of volatile and refractory elements are consistent with mixing and do not show the scatter expected from a fractional vaporization process. We conclude that fractional vaporization had little or no role in producing the observed liquid trend, except in the loss of CO_2.

The glass composition range can, on the other hand, be modelled as a mixing line[30] between two endmember compositions. Figure 3 shows that the hypothesis of mixing two rock compositions to produce the glass range is consistent with the observed correlations of log ratios in the Beloc glasses, and that the correlation coefficients are very good. Although the high-Ca and intermediate data points approximate linear compositional

◀ FIG. 2 Oxide variation diagrams for Beloc glasses, including all individual electron microprobe analyses, showing *a*, CaO and Al_2O_3 plotted against SiO_2, *b*, MgO and K_2O plotted against SiO_2 and *c*, FeO* and TiO_2 plotted against SiO_2.

TABLE 1 Composition of Beloc average glass, glass endmembers and calculated 'marl' and 'mudrock' target

	BE4-242 glass*	BE4-242 +CO_2	Mudrock'	Argillite	BE4-42 glass*	Average Beloc glass
SiO_2	44.44	36.27	62.8	60.5	67.48	63.09 ± 2.13
TiO_2	0.66	0.54	0.9	0.4	0.61	0.67 ± 0.07
Al_2O_3	11.72	9.56	16.6	18.1	15.14	15.21 ± 0.31
FeO†	4.8	3.92	6.8	7.5	4.30	5.44 ± 0.38
MnO	0.1	0.08	0.1	0.1	0.21	0.14 ± 0.05
MgO	4.41	3.6	6.2	4.6	2.26	2.74 ± 0.30
CaO	30.71	25.07	2.4	1.6	4.98	7.26 ± 1.72
Na_2O	2.01	1.64	2.8	4.4	3.52	3.63 ± 0.27
K_2O	0.48	0.39	0.7	2.5	1.76	1.59 ± 0.12
CO_2	—	18.59				
Sum	99.32				100.25	99.76

BE4-242 glass, yellow-coloured beloc glass, the rare and most calcic endmember of the glass trend; BE4-242 + CO_2, hypothetical marl composition calculated from calcic glass BE4-242 with CO_2 added to form $CaCO_3$ with 29 wt% of the CaO present; 'Mudrock', hypothetical 'mudrock' composition calculated by subtraction of $CaCO_3$ (all CO_2 and stochiometrically equivalent CaO) from column 2; Argillite, a natural mudrock, from Keweenawan, Canada, renormalized to 100%[31]; BE4-42 glass, black glass, the high-silica endmember of the Beloc glass trend. Average composition of Beloc glasses: mean of 61 electron microprobe analyses, with standard deviation (1σ). Average does not include the rare high-Ca glasses. Trace-element content (p.p.m.) of bulk glass (neutron activation analysis) is: Ni < 85; Cr = 23.7; Co = 13.1; Sc = 19.2; As = 3.3; Br < 0.5; W < 1.5; Sb < 0.18; Rb = 54.0; Cs = 0.97; Ba = 410; Zr = 162; Hf = 3.87, Ta = 0.43; La = 22.3; Ce = 47.7; Nd = 21; Sm = 5.02; Eu = 1.19; Tb = 0.70; Yb = 2.89; Lu = 0.43; Th = 6.35; U = 1.1.

* Electron microprobe analyses.

† Total Fe reported as FeO.

trends, there is significant curvature at the high-SiO_2 end, for example in the CaO trend in Fig. 2*a*. These deviations from linearity may reflect significant compositional variation within the impact terrain that gave rise to the black glass.

Nature of the impact terrain

Although the mixing model provides a very satisfactory numerical solution, it is not geologically reasonable because the high-CaO endmember is a rock composition not known on Earth. The source terrain that generated this high-CaO melt may have been chemically modified by the melting process, however, due to the loss of a volatile CO_2 component from a geologically realistic rock composition such as marl or interbedded limestones and shales. Thus the most calcic glass could be considered the product of fusion of marl, composed of a mixture of mudrock and $CaCO_3$, accompanied by loss of CO_2 before quenching to glass. The degassing of CO_2 from the melt may account for the high vesicularity of the Ca-rich yellow glasses. The composition of a 'marl' produced by the mixture of CO_2 and the high-Ca Beloc glass is shown in column 2 of Table 1, after addition of the CO_2 required to balance most of the CaO. The 'mudrock' composition (the rock resulting from removal of the $CaCO_3$) is shown in column 3, and it may be compared to the mudrock or argillite in column 4. This calculated 'mudrock' is comparable to the composition of common mudrock[31,32], with the exception of a slightly higher MgO and a higher Na/K ratio.

Although the melting of a marl source rock can account for the derivation of the high-Ca glass by vaporization of CO_2 and generation of the Beloc glass trend by mixing, the origin of the silicic endmember cannot be attributed to a mudrock source of this composition. The silicic glasses are much lower in MgO than typical mudrock, and have higher Fe/Mg ratio and lower Na/K ratio, as shown in Table 1. The silicic glasses have incompatible element and REE content typical of upper continental crust, such as australites, Ivory Coast tektites, deep-sea turbidites and calc-alkaline andesites, but show uniquely high K/Cs and high Th/U. They could be derived from the complete melting of upper continental crust of broadly granitic composition. The range of glass compositions found at the K/T boundary in Beloc is thus consistent with an impact melt that is dominantly derived from upper continental crustal rocks of granitic or andesitic type, with a minor contribution from the melting of marl. A granitic source is also consistent with the shocked mineral assemblage found in the impact layer at the K/T boundary[33], but the Beloc glass data and shocked mineral assemblage are both inconsistent with the oceanic crustal source of the impact proposed in a number of studies[12,34]. The glass data are consistent with an impact site on continental crust overlain by marl sediment, such as on a continental shelf or slope. A location of the K/T boundary impact at the Manson impact structure in Iowa has been proposed by several workers[8,35]. This impact terrain is consistent with the available evidence from the Beloc glasses, as the central uplift of the Manson structure consists of lower and middle Proterozoic granite and gneiss[36], overlain by deformed Cretaceous marine shale and limestone[37,38]. Another

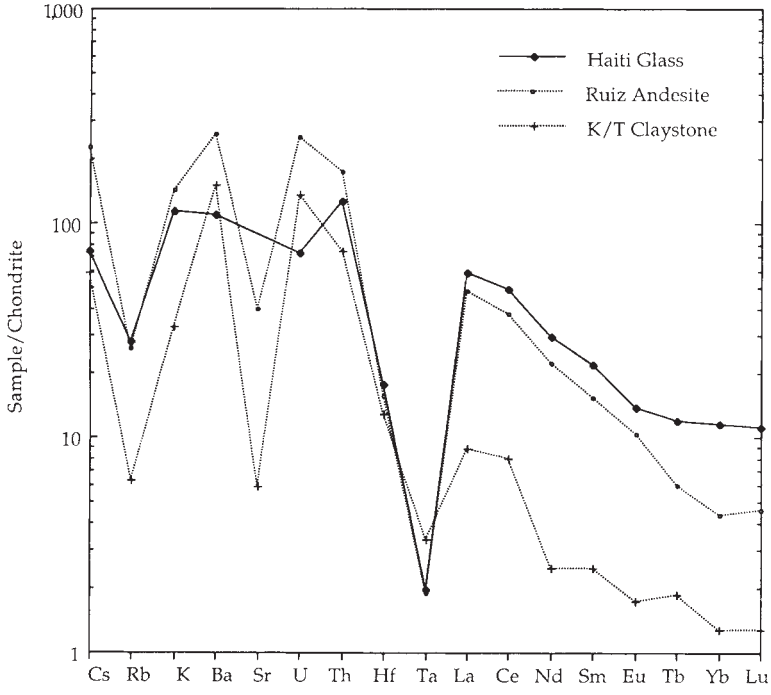

FIG. 3 Logarithmic plots of the oxide ratios of Beloc glasses showing high degree of correlation between *a*, ln (K_2O/CaO) and ln (SiO_2/MgO), and *b*, between ln (MgO/K_2O) and ln (CaO/Na_2O), consistent with an origin of the compositional trend by the mixing of two endmember compositions. The equations of the regression lines are: *a*, $y = -10.5 + 2.86x$, $r^2 = 0.967$; *b*, $y = 2.38 \times 10^{-2} - 0.78\ x$, $r^2 = 0.976$. The glass compositions in middle of the trend occur as streaks in the high-silica glass (Fig. 1*c*).

possible site of the K/T impact has been proposed on the Yucatan peninsula in Mexico[39]. We note that the 180-km-diameter Yucatan feature also has a geological succession of the type that could generate the observed Haiti glass compositions, with andesitic rocks, marls and a 80-m-thick bentonitic calcareous breccia. A detailed geochemical comparative study of Beloc glasses and Yucatan and Manson rocks is needed to evaluate these possible impact sites.

The claystone at the K/T boundary in western United States contains common spherules of kaolinite[8], and the suggestion has been made that the claystone is the product of alteration from glass[9]. Comparison of the chemical composition of Beloc glasses with the K/T boundary claystone are complicated by the mobility of a number of elements during alteration and diagenesis of the claystone. It has been proposed[8,34] that the Ti/Al ratio in the claystone (0.047 ± 0.005, 1σ error) reflects that of the progenitor rock and has remained unaffected by diagenesis. The mean Ti/Al ratio in Beloc glasses is 0.050 ± 0.005 (1σ), identical within analytical error. The trace-element distribution in the Beloc glass is compared with that of the K/T boundary claystone in Fig. 4. Although the REE patterns are very similar, the K/T boundary claystone is depleted in all the rare earths by an order of magnitude compared with the Beloc glasses. A comparable relationship has been observed during the alteration of volcanic glass to clay, where the REEs are strongly depleted overall, but the shape of the chondrite-normalized pattern remains unchanged[40,41]. The larger cations (Cs, Rb, K) are depleted in the claystone relative to the Beloc glasses, as would be expected during alteration to clay, whereas the content of hafnium, an element that is immobile during alteration of volcanic glass to clay, is identical[41]. Finally, both Beloc glasses and the claystone have very low Ni and Cr content, lower than typical shale. The geochemical evidence is thus consistent with a genetic relationship between the K/T boundary claystone and the Beloc tektite-like glass.

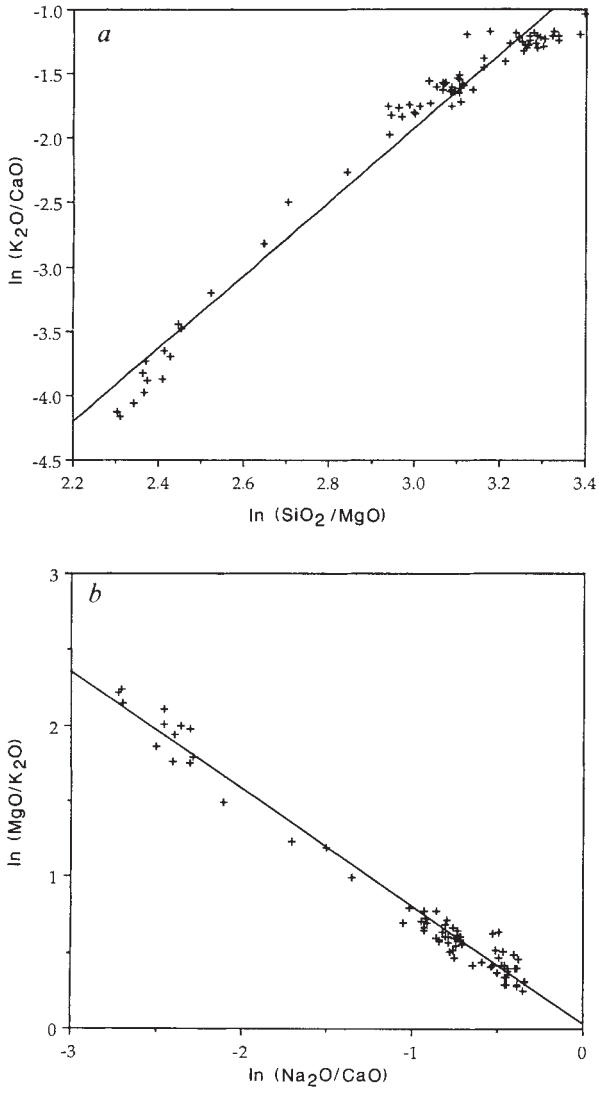

FIG. 4 Chondrite-normalized distribution of trace elements in Beloc glass, compared to K/T boundary claystone from the Raton basin[8] and Nevado del Ruiz andesite[43]. The elements are normalized to Leedy chondrite and basalt KD11[44,45]. The Beloc trace-element data are given in the Table 1 legend.

If the Beloc glasses are the precursor to the claystone band observed in K/T boundary marine and continental sediments, then the composition of the Haiti glasses can provide clues to the relative mass of impact ejecta and the nature of the volatile fraction released to the atmosphere. Glass constitutes a minimum of 25% of the Beloc layer, but may have constituted up to 58% if the associated smectite is its alteration product. The total glass fraction is a minimum of 0.5 g cm^{-3}, and the yellow glass content is ~2%, or 10 mg cm^{-3}. In keeping with the marl hypothesis discussed above, ~23% of the marl (3 mg cm^{-3}) was lost as CO_2 during vaporization; thus the total fraction of marl represented in the impact layer and released to the atmosphere is 13 mg cm^{-3}. If we adopt a 1-cm global mean thickness of the claystone layer as a conservative estimate[8], the total global glass fallout, based on the mass fraction (500 mg cm^{-3}) in the Beloc sediment, is 2.5×10^{15} kg, corresponding to ~1,000 km^3 or rock. For a bolide mass of 0.6×10^{15} kg (ref. 1), the impact ejecta mass has been estimated to be 5–200 times the bolide mass[42], or in the range 10^3–4×10^4 km^3. Our minimum estimate of ~1,000 km^3 is at the lower end of this range. The yellow-glass component of the global fallout layer is estimated as 5×10^{13} kg (20 km^3 rock) on the basis of its abundance in the Beloc section, on a CO_2-free basis. The CO_2 liberated to the atmosphere from the proposed marl at the time of impact would constitute another 4.6 km^3. All of the above are minimum estimates, and could be low by a factor of four. Thus we estimate the total 'marl' involved in the impact, as yellow glass in the ejecta layer and as CO_2 in the atmosphere, to be about 25 km^3. The above calculations imply that about 10^{16} g or 8×10^{14} moles of CO_2 were emitted to the atmosphere at the time of the impact. This is about three times the estimated annual CO_2 release during Deccan flood-basalt volcanism[3] and is comparable to the current annual anthropogenic output. Regardless of the implications for environmental effects from the direct release of CO_2 from impacted material, the glass occurring in the Haiti layer provides direct evidence for a major continental impact at the K/T boundary. □

Received 26 November 1990; accepted 15 January 1991.

1. Alvarez, L. W., Alvarez, W., Asaro, F. & Michel, H. V. *Science* **208,** 1095–1108 (1980).
2. McLean, D. M. *Cretac. Res.* **6,** 235–259 (1985).
3. Officer, C. B., Hallam, A., Drake, C. L. & Devine, J. D. *Nature* **326,** 143–149 (1987).
4. Smit, J. & Klaver, G. *Nature* **292,** 47–49 (1981).
5. Smit, J. *Geologie Mijnb.* **69,** 187–204 (1990).
6. Bohor, B. F., Triplehorn, D. M., Nichols, D. J. & Millard, H. T. Jr *Geology* **15,** 896–899 (1987).
7. Izett, G. A. *Geol. Soc. Am. Bull.* **99,** 78–86 (1987).
8. Izett, G. A. *Spec. Pap. geol. Soc. Am.* **249,** (1990).
9. Pollastro, R. M., Pillmore, C. L., Tschudy, R. H., Orth, C. J. & Gilmore, J. S. *32nd A. Clay Minerals Conf.* Program and Abstracts, 83 (Clay Minerals Soc., Buffalo, 1983).
10. Pollastro, R. M. & Pillmore, C. L. *J. sedim. Petrol.* **57,** 456–466 (1987).
11. Shaw, H. F. & Wasserburg, G. J. *Earth planet. Sci. Lett.* **60,** 155–177 (1982).
12. DePaolo D. J., Kyte, F. T., Marshall, B. D., O'Neill, J. R. & Smit, J. *Earth planet. Sci. Lett.* **64,** 356–373 (1983).
13. Alvarez, W. *Eos* **71,** 1424 (1990).
14. Hildebrand, A. R. & Boynton, W. V. *Eos* **71,** 1424 (1990).
15. Hildebrand, A. R. & Boynton, W. V. *Science* **248,** 843–847 (1990).
16. Maurasse, F. J. M. R. *Guide to the Field Excursions of Haiti* (Miami Geol. Soc., Miami, 1982).
17. Jiang, M. J. & Gartner, S. *Micropaleontology* **32,** 232–255 (1986).
18. Martini, E. *Proc. 2nd Plankton Conf.* (ed. Farinacci, A.) 736–785 (Edizioni Tecnoscienza, Rome, 1971).
19. Alvarez, W. *et al. Geol. Soc. Am. Bull.* **88,** 367–389 (1977).
20. Berggren, W. A., Kent, D. V. & Flynn, J. J. *Mem. geol. Soc. Lond.* **10,** 141–195 (1985).
21. Monechi, S. & Thierstein, H. R. *Mar. Micropaleont.* **9,** 419–440 (1985).

22. Chapman, D. R. & Scheiber, L. C. *J. geophys. Res.* **74,** 6737–6776 (1969).
23. McLennan, S. M., Taylor, S. R., McCulloch, M. T. & Maynard, J. B. *Geochim. cosmochim. Acta* **54,** 2015–2050 (1990).
24. D'Hondt, S. L., Keller, G. & Stallard, R. F. *Meteoritics* **22,** 61–79 (1987).
25. Schnetzler, C. C., Philpotts, J. A. & Thomas, H. H. *Geochim. cosmochim. Acta* **31,** 1987–1993 (1967).
26. Engelhardt, W. V., Luft, E., Arndt, J., Schock, H. & Weiskirchner, W. *Geochim. cosmochim. Acta* **51,** 1425–1443 (1987).
27. Taylor, S. R. & White, A. J. R. *Bull. Volcan.* **29,** 177–194 (1966).
28. Walter, L. S. & Guitronich, J. E. *Solar Energy* **9,** 163–169 (1967).
29. Walter, L. S. *Geochim. cosmochim. Acta* **31,** 2043–2063 (1967).
30. Delano, J. W. & Lindsley, D. H. *Geochim. cosmochim. Acta* **46,** 2447–2452 (1982).
31. MacPherson, H. G. *Geochim. cosmochim. Acta* **14** 76 (1958).
32. Blatt, H., Middleton, G. & Murray, R. *Origin of Sedimentary Rocks* 2nd edn (Prentice-Hall, Englewood Cliffs, 1980).
33. Bohor, B. F., Foord, E. E., Modreski, P. J. & Triplehorn, D. M. *Science* **224,** 867–869 (1984).
34. Gilmore, J. S., Knight, J. D., Orth, C. J., Pillmore, C. L. & Tschudy, R. H. *Nature* **307,** 224–228 (1984).
35. French, B. M. *Science* **226,** 353 (1984).
36. Sims, P. K. *U.S. Geol. Surv. Open File Rep.* 85-0604 (1985).
37. Smith, T. A. thesis, Iowa State Univ. (1971).
38. Hartnung, J. B. & Anderson R. R. *Lunar planet. Inst. Tech. Rep.* 88-08 (1988).
39. Hildebrand, A. R. & Penfield, G. T. *Eos* **71,** 1425 (1990).
40. Zielinski, R. A. *Chem. Geol.* **35,** 185–204 (1982).
41. Zielinski, R. A. *Sedimentology* **32,** 567–579 (1985).
42. O'Keefe, J. D. & Ahrens, T. J. *Lunar planet. Sci.* **19,** 883–884 (1988).
43. Melson, W. G. *et al. J. Volcan. geotherm. Res.* **41,** 97–126 (1990).
44. Kay, R. W. & Hubbard, N. *Earth planet. Sci. Lett.* **38,** 95–111 (1978).
45. Kay, S. M. *J. geophys. Res.* **92,** 6173–6189 (1987).

ACKNOWLEDGEMENTS. We thank J. Gardner for determination of the trace-element composition of glasses by neutron activation analysis at the Nuclear Research Center, University of Rhode Island. We thank J. Devine for the determination of major-element composition of glasses by electron microprobe analysis at Brown University.

Requirement of the RNA helicase-like protein PRP22 for release of messenger RNA from spliceosomes

Mahshid Company, Jaime Arenas & John Abelson

Division of Biology, California Institute of Technology, Pasadena, California 91125, USA

The product of the yeast *PRP22* gene acts late in the splicing of yeast pre-messenger RNA, mediating the release of the spliced mRNA from the spliceosome. The predicted PRP22 protein sequence shares extensive homology with that of PRP2 and PRP16 proteins, which are also involved in nuclear pre-mRNA splicing. The homologous region contains sequence elements characteristic of several demonstrated or putative ATP-dependent RNA helicases. A putative RNA-binding motif originally identified in bacterial ribosomal protein S1 and *Escherichia coli* polynucleotide phosphorylase has also been found in PRP22.

NUCLEAR pre-mRNA splicing takes place on a large particle, the spliceosome[1–3], whose function is to fold the pre-mRNA into a substrate for splicing and to catalyse the reaction. The splicing reaction itself consists of two phosphotransfer reactions. In mechanism, it is identical to that of the type II self-splicing introns (for a review see refs 4–7). It is therefore widely believed that pre-mRNA splicing is also an RNA-catalysed reaction. Despite that conviction, ATP hydrolysis is required for most of the discernible steps in spliceosome assembly as well as for each of the two phosphotransfer reactions[8–14].

The components of the spliceosome include four small nuclear ribonucleoprotein particles (snRNPs) (U1, U2, U4/U6, and U5) and numerous proteins (for a review see refs 15–21). Many of these proteins have been defined through the isolation of temperature sensitive (ts) *prp* mutants (for pre-RNA processing) in *Saccharomyces cerevisiae* (reviewed in refs 19–21). At the nonpermissive temperature these mutants block pre-mRNA splicing *in vivo* resulting in various phenotypes. Most accumulate pre-mRNA but at least three of them accumulate the splicing intermediates and two others splice normally but accumulate introns in lariat form. One mutant, *prp22*, the subject of this report, accumulates both intron and pre-mRNA at the nonpermissive temperature.

There are now at least 21 known classes of *prp* mutants (*prp2–prp9, prp11, and prp16–prp28*). *In vitro* analysis of extracts prepared from a number of *prp* mutants indicates that the PRP gene products are directly involved in the mRNA splicing process[13,22]. Some are integral snRNP proteins, including PRP8 (ref. 23), which is part of the U5 snRNP and for which a mammalian analogue[24,25] has been identified, and PRP4, part of the U4/U6 snRNP (refs 26, 27). None of the 8–10 sm core proteins, integral components of each of the four mammalian snRNPs, have yet been identified as *prp* mutants. Other proteins, for example PRP11, are associated with the spliceosome but not specifically with any snRNP (ref. 28). Some PRP proteins, for example, PRP5, PRP6, PRP9, and PRP11, are required at early stages of spliceosome assembly whereas others, for example PRP2, PRP16, PRP17, PRP18 and PRP22, act on the fully assembled spliceosome (see review in ref. 21).

The sequences of most of the *PRP* genes have been determined and in some cases they give a clue to the function of the gene product. We have been especially interested in a set of proteins whose sequences are homologous to a growing group of ATP-dependent RNA helicases epitomized by the eukaryotic protein synthesis initiation factor eIF4A (refs 29–34). Both PRP5 and PRP16 are members of this group[35,36]. The involvement of these proteins in splicing could explain the role of ATP hydrolysis in spliceosome assembly and in the reaction itself.

Here we demonstrate, through the analysis of splicing in heat-treated extracts, that PRP22 is required for the release of the mRNA product from the spliceosome, a previously unsuspected step. We have cloned and sequenced the *PRP22* gene. The protein sequence is highly homologous to that of PRP16 (ref. 36) and the recently sequenced PRP2 (ref. 37). These three PRP proteins define a novel family of RNA helicase-like genes which mediate three consecutive steps late in the mRNA splicing pathway.

Heat inactivation of PRP22 splicing extract

Heat inactivation of splicing extracts prepared from many *prp* mutant strains has suggested a direct role for the PRP gene products in pre-mRNA splicing[22]. Extracts were prepared from a *prp22* ts strain grown at the permissive temperature (23 °C). Heat lability of splicing activity in this extract was investigated